INTERNATIONAL JOURNAL OF CLIMATOLOGY
Int. J. Climatol. **20**: 641–661 (2000)

PRECIPITATION PREDICTORS FOR DOWNSCALING: OBSERVED AND GENERAL CIRCULATION MODEL RELATIONSHIPS

R.L. WILBY[a,b,*] and T.M.L. WIGLEY[a]
[a] *National Center for Atmospheric Research, Boulder CO, 80303, USA*
[b] *Division of Geography, University of Derby, Kedleston Road, Derby, DE22 1GB, UK*

Received 18 August 1998
Revised 28 August 1999
Accepted 9 September 1999

ABSTRACT

Because of the coarse resolution of general circulation models (GCM), 'downscaling' techniques have emerged as a means of relating meso-scale atmospheric variables to grid- and sub-grid-scale surface variables. This study investigates these relationships. As a precursor, inter-variable correlations were investigated within a suite of 15 potential downscaling predictor variables on a daily time-scale for six regions in the conterminous USA, and observed correlations were compared with those based on the HadCM2 coupled ocean/atmosphere GCM. A comparison was then made of observed and model correlations between daily precipitation occurrence (a time series of zeroes and ones) and wet-day amounts and the 15 predictors. These two analyses provided new insights into model performance and provide results that are central to the choice of predictor variables in downscaling of daily precipitation. Also determined were the spatial character of relationships between observed daily precipitation and both mean sea-level pressure (mslp) and atmospheric moisture and daily precipitation for selected regions. The question of whether the same relationships are replicated by HadCM2 was also examined. This allowed the assessment of the spatial consistency of key predictor–predictand relationships in observed and HadCM2 data. Finally, the temporal stability of these relationships in the GCM was examined. Little difference between results for 1980–1999 and 2080–2099 was observed.

For correlations between predictor variables, observed and model results were generally similar, providing strong evidence of the overall physical realism of the model. For correlations with precipitation, the results are less satisfactory. For example, model precipitation is more strongly dependent on surface divergence and specific humidity than observed precipitation, while the latter has a stronger link to 500 hPa divergence than is evident in the model. These results suggest possible deficiencies in the model precipitation process, and may indicate that the model overestimates future changes in precipitation. Correlation field patterns for mslp versus precipitation are remarkably similar for observed data and HadCM2 output. Differences in the correlation fields for specific humidity are more noticeable, especially in summer. In many cases, maximum correlations between precipitation and mslp occurred away from the grid box; whereas correlations with specific humidity were largest when the data were propinquitous. This suggests that the choice of predictor variable and the corresponding predictor domain, in terms of location and spatial extent, are critical factors affecting the realism and stability of downscaled precipitation scenarios. Copyright © 2000 Royal Meteorological Society.

KEY WORDS: North America; statistical downscaling; general circulation models (GCM); validation; precipitation

1. INTRODUCTION

It is widely acknowledged that the direct outputs of climate change simulations from general circulation models (GCMs) are inadequate for assessing land-surface impacts on *regional scales* (DOE, 1996). This is primarily for two reasons: first, because the spatial resolution of GCMs (typically 50000 km^2) is often larger than that required for input to impacts models; and second, because of doubts about the reliability of some GCM output variables (particularly those, like precipitation, that are critically dependent on

* Correspondence to: Division of Geography, University of Derby, Kedleston Road, Derby, DE22 1GB, UK; tel: +44 1332 591 726; fax: +44 1332 622 747; e-mail: r.l.wilby@derby.ac.uk

Copyright © 2000 Royal Meteorological Society

sub-grid-scale processes such as those involving clouds). This leads to a scale mismatch between the information that GCMs are able to supply most confidently and that which is generally required by the climate change impacts community (e.g. Hostetler, 1994). Consequently, statistical 'downscaling' techniques have emerged as a means of relating meso-scale GCM output (frequently atmospheric circulation data) to sub-grid-scale surface variables (such as precipitation), under the assumption that the former GCM outputs are more reliable than the latter.

Statistical downscaling, therefore, is based on the assumptions that (i) suitable relationships can be developed between grid- and larger-scale versus grid- and smaller-scale predictor variables; (ii) these observed, empirical relationships are valid under future climate conditions; and (iii) the predictor variables and their changes are well characterised by GCMs. If these assumptions hold, it is then possible to produce scenarios of regional and smaller-scale climate from future climate change data produced by GCMs, that are both more reliable and of finer resolution than the 'raw' GCM data.

The theory and practice of statistical downscaling are well described in the literature (e.g. Kim *et al*., 1984; Karl *et al*., 1990; Wigley *et al*., 1990; Giorgi and Mearns, 1991; von Storch *et al*., 1993; Wilby and Wigley, 1997). However, there is little consensus among such studies as to the choice of atmospheric predictor variables. For example, Table I shows some of the wide variety of downscaling predictors that have been employed in recent studies of daily precipitation. From this limited sample, it is evident that there has been a tendency to use circulation data as predictors, although a smaller sub-set of papers has stressed the value of incorporating atmospheric moisture and other variables in downscaling schemes (e.g. Karl *et al*., 1990; Crane and Hewitson, 1998; Charles *et al*., 1999). Since the explanatory power of any given predictor will vary both spatially and temporally (e.g. Huth, 1999), the results of an objective comparison of different predictors and their spatial character should be a useful addition to current downscaling research.

The goal of the present paper is to throw some light on the choice of predictor variables in regression-based (or similar) downscaling methods. In previous studies, it was rare to find any

Table I. Downscaling daily precipitation: predictor variables and techniques used in recent studies

Author(s)	Predictor variable(s)	Technique(s)
Bardossy and Plate (1992)	500 hPa heights	Weather classification
Conway *et al.* (1996)	Vorticity	Semi-stochastic, regression and resampling
Crane and Hewitson (1998)	Geopotential heights, specific humidity	Artificial neural nets
Goodess and Palutikof (1998)	Mean sea-level pressure, airflow indices	Weather classification
Hay *et al.* (1992)	Wind direction, cloud cover	Weather classification
Karl *et al.* (1990)	Geopotential heights and thicknesses, sea-level pressure, relative humidity	Principal Components Analysis and Canonical Correlation
Katz and Parlange (1996)	Sea-level pressure anomalies	Stochastic
Kilsby *et al.* (1998)	Vorticity, sea-level pressure, airflow strength and direction, altitude, distance from coast, grid reference	Regression
Matyasovszky and Bogardi (1996)	500 & 700 hPa heights	Weather classification
Perica and Foufoula-Georgiou (1996)	Thermodynamic parameters	Stochastic-dynamic
Wilby (1998)	Vorticity, sea surface temperature anomalies, North Atlantic Oscillation index	Semi-stochastic, regression
Wilks (1992)	Monthly precipitation	Stochastic
Woodhouse (1997)	Teleconnection indices	Rotated Principal Components Analysis

Copyright © 2000 Royal Meteorological Society

comprehensive assessment of a range of possible predictors, and equally rare to see results where the strengths of individual predictor–predictand correlations are documented. Both aspects are considered here. Furthermore, while such downscaling work is predicated on the assumption that GCMs can provide credible 'forcing' data for driving relationships derived from observed data, GCMs have rarely, if ever, been validated in ways that mesh with their application to downscaling. This deficiency will be remedied by exploring a number of new methods for GCM validation.

2. METHODS

2.1. Data sources

The GCM used was the UK Meteorological Office, Hadley Centre's coupled ocean/atmosphere model (HadCM2) forced by combined CO_2 and albedo (as a proxy for sulphate aerosol, SUL) changes (Johns *et al.*, 1997; Mitchell and Johns, 1997). In this 'SUL' experiment, the model run begins in 1861 and is forced with an estimate of historical forcing to 1990 and a projected future forcing scenario over 1990–2100. The historical forcing is only an approximation of the 'true' forcing, with the result that the GCM results for model years 1980–1999, for example, would not be expected to represent present-day conditions exactly (see Appendix A in Wilby *et al.*, 1998b). Nonetheless, HadCM2 output for 1980–1999 has been employed as a proxy of the present climate for downscaling daily precipitation, temperature, humidity, sunshine totals and wind speeds in selected regions of the USA (Wilby *et al.*, 1998b), Europe (Conway *et al.*, 1996) and Japan (Wilby *et al.*, 1998a).

In the present study, observed and HadCM2 daily precipitation data were evaluated for six climatically distinct regions in the USA (Figure 1 and Table II) centred on: (i) 45°N/123.75°W [Salem, Oregon; abbreviated SLM]; (ii) 40°N/120°W [Sierra Nevada, CA; SNV]; (iii) 35°N/97.5°W [Oklahoma City, OK; OKC]; (iv) 45°N/93.75°W [Minneapolis, MA; MSP]; (v) 32.5°N/90°W [Jackson, MS; JKS]; and (vi) 40°N/75°W [Philadelphia, PA; PHL]. The HadCM2 precipitation data were provided by the Hadley

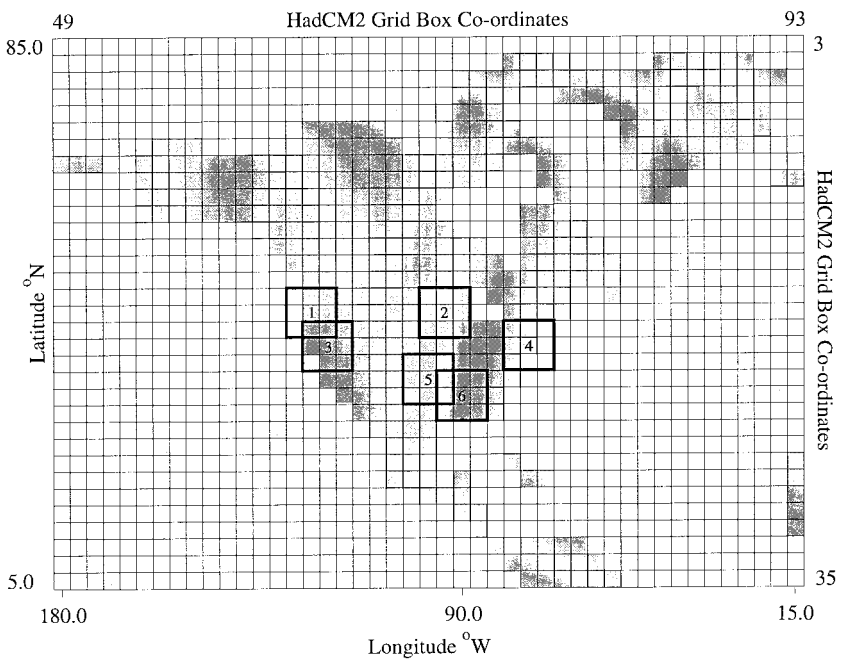

Figure 1. Location of the six downscaling study regions in relation to the HadCM2 North American grid boxes. Refer to Table II for individual site details. Note that the bold (3 × 3) boxes correspond to the domains used for calculating the daily vorticity, divergence, geostrophic wind speed and direction

Copyright © 2000 Royal Meteorological Society

Table II. Downscaling study regions: central latitudes and longitudes for the primary HadCM2 grid boxes together with an identifying geographical location

Abbreviation	Latitude	Longitude	Location
1 SLM	45°N	123.75°W	Salem, OR
2 MSP	45°N	93.75°W	Minneapolis, MN
3 SNV	40°N	120°W	Sierra Nevada. CA
4 PHL	40°N	75°W	Philadelphia, PA
5 OKC	35°N	97.5°W	Oklahoma City, OK
6 JKS	32.5°N	90°W	Jackson, MS

Centre for the model years 1980–1999 and 2080–2099 (D. Viner, personal communication, UK Climate LINK project, Climatic Research Unit).

Observed daily precipitation, maximum (T_{max}) and minimum (T_{min}) temperature series were obtained for five stations in each of the six central grid boxes shown in Figure 1. The grid box average was calculated using the unweighted mean of the daily totals at the five sites. The 'target' regions were 2.5° latitude by 3.75° longitude grid boxes corresponding to the HadCM2 grid. The station data were obtained from the US National Climatic Data Center (NCDC) archive. The chosen analysis period (1979–1995) corresponds to the availability of NCEP (National Center for Environmental Prediction) re-analysis data (Kalnay *et al*., 1996) at the time this study was initiated (see below).

Parallel sets of explanatory variables were obtained from HadCM2 (1980–1999) and re-analysis data (see Table III). Daily grid-point data for mean sea-level pressure (mslp) and 500 hPa geopotential heights (H_{500}) for the entire North American field, including points centred on each of the six study regions, were taken from the NCEP re-analysis for the period 1979–1995, and re-gridded to the HadCM2 grid. Daily grid-point vorticity (Z_s), geostrophic flow strength (F_s), flow velocity (resolved into zonal (U_s) and meridional (V_s) components), and divergence (D_s) were calculated for each grid-point using both HadCM2 and re-analysis daily mslp. Equivalent circulation indices (i.e. Z_{500}, F_{500}, U_{500}, V_{500} and D_{500}) were also calculated for the upper atmosphere using the HadCM2 and re-analysis 500 hPa geopotential heights. The first three indices (i.e. mean sea-level vorticity, geostrophic flow strength and direction of flow) have been employed by Jones *et al*. (1993) and Hulme *et al*. (1993) in developing an objective weather typing system for the British Isles, and have since been applied in several statistical downscaling studies (e.g. Conway *et al*., 1996; Kilsby *et al*., 1998; Pilling *et al*., 1998; Wilby *et al*., 1998b).

Table III. Definition of predictor variables

Predictors	Abbreviation
Surface variables	
Specific humidity (g/kg)	q
Maximum temperature (°C)	T_{max}
Minimum temperature (°C)	T_{min}
Mean sea-level pressure (hPa)	mslp
Zonal velocity component	U_s
Meridional velocity component	V_s
Strength of the resultant flow (hPa)	F_s
Vorticity (hPa)	Z_s
Divergence (hPa)	D_s
Upper-atmosphere variables (500 hPa)	
500 hPa geopotential height (m)	H_{500}
Vorticity (hPa)	Z_{500}
Strength of the resultant flow (hPa)	F_{500}
Zonal velocity component	U_{500}
Meridional velocity component	V_{500}
Divergence (hPa)	D_{500}

Copyright © 2000 Royal Meteorological Society

Finally, daily maximum (T_{max}), minimum (T_{min}) and mean temperatures were obtained for the six target regions from HadCM2 output (using the 1980–1999 means of daily T_{max} and T_{min}). (Note that, for the observations, station temperature data were employed rather than re-analysis data, since these were considered to be more reliable. However, the daily station means and re-analysis data are highly correlated). In addition, daily mean surface relative humidity and 0.995 sigma level relative humidity were obtained for all regions using both HadCM2 (1980–1999) and re-analysis (1979–1995) output. In both cases, because specific humidity (q) has been shown to be a valuable downscaling predictor (Crane and Hewitson, 1998), daily mean temperatures and relative humidities were used to estimate daily mean specific humidities using Richards' (1971) non-linear approximation. This estimation procedure was necessary because only relative humidity had been archived at daily time-steps for the HadCM2 experiment.

2.2. Methods of analysis

Relationships between the 15 predictor variables (listed in Table III), daily time series of precipitation occurrence ($O_i = 0$ if dry, $O_i = 1$ if wet) and wet-day amounts (R_i in mm/day) were investigated using two methods; by examining propinquitous (i.e. same location) relationships, and by examining relationships where the predictors were spatially remote from the predictands. Following Karl *et al.* (1990), predictor variables were chosen that were expected to be important in predicting daily rainfall (under the constraint of limitation to variables for which HadCM2 data were archived). The choice of predictors also broadly reflects those most commonly employed in recent statistical downscaling studies (Table I). For the predictand, rather than using precipitation as a continuous daily time series, data were split into dry and wet days and a separate examination took place of the occurrence series, O_i (i.e. a time series of zeroes and ones), and the wet-day amounts series, R_i (i.e. ignoring dry days). This allows the results of the present analyses to be transferred more directly to weather generator and downscaling applications than similar previous analyses.

Inter-relationships were first examined between the predictor variables for each region, for winter (December, January, February, DJF) and summer (June, July, August, JJA), and for observed (NCEP) and model (HadCM2) data using standard product-moment correlation coefficients. This analysis allows a determination of which predictors are most strongly correlated, which in turn helps in making a parsimonious selection of predictors for downscaling. These results can also assist in choosing a set of quasi-independent predictor variables that will reduce the problem of multicollinearity in developing regression equations. Comparing observed and HadCM2 results provides a means of validating the GCM—few, if any, such tests of the internal consistency of GCMs have been carried out before.

Following this, predictor–precipitation correlations were computed for each region using observed and HadCM2 data, for winter (DJF) and summer (JJA), using grid box, area-average precipitation (O_i and R_i). For each region and season the strongest (negative and positive) correlations were identified, and the percentage of variance in O_i or R_i explained by each predictor was calculated. This procedure identifies the most powerful predictor variables by site and season. It also quantifies similarities and differences between the observed and HadCM2 predictor–precipitation relationships, thus providing a further means of validating the GCM.

Finally, the spatial patterns of correlations between daily precipitation (O_i and R_i) and two of the predictor set variables (daily mslp and specific humidity) were determined to obtain some insight into the degree of propinquity in correlations involving these variables. (Similar analyses, using 700 hPa height data, have been carried out by Stidd, 1954; Klein, 1963 and McCabe and Dettinger 1995.) Daily mslp was selected for analysis because it is the basis of derived variables such as surface vorticity, airflow strength, meridional and zonal flow components, and divergence, and is readily interpretable in terms of the continental-scale atmospheric circulation. Similarly, daily specific humidity was chosen because of the reported significance of this variable to GCM precipitation schemes (e.g. Hennessy *et al.*, 1997). This type of pattern analysis identifies the optimum predictor domain (spatial extent and position) for the chosen predictor variable and downscaling region. In carrying out these pattern analyses with both observed and

Copyright © 2000 Royal Meteorological Society

HadCM2 data, yet another means of validating the GCM is provided. If the correlation fields are similar, then HadCM2 precipitation is being forced by realistic linkages to atmospheric circulation, which in turn means that downscaled precipitation scenarios using circulation indices should be consistent with observed data.

Ideally, these correlation pattern analyses should be undertaken for all combinations of regions, seasons and predictor variables. However, for illustrative purposes, the present analysis was restricted to the correlation fields for mslp and q versus grid box area-average O_i (occurrence) and R_i (wet-day amounts) only at Sierra Nevada (SNV) and Oklahoma (OKC) in summer and winter. The SNV grid box was selected because of its relative proximity to an oceanic moisture source and the strong orographic component to its rainfall. In contrast, the OKC grid box was chosen because of its relative continentality and limited orographic influences. At this point, the analyses are not intended to be definitive, but instead are meant to demonstrate a technique that can assist in the choice of downscaling predictor variables and domain size. Note that area-average precipitation data are used for these analyses in order to maintain correspondence between observed and GCM analyses.

3. RESULTS

3.1. Predictor variable correlations

Table IV lists the strongest inter-variable correlations, on a daily scale, arising from the analysis of propinquitous predictor variables and lumping all regions together. Given the large sample sizes, correlation coefficients exceeding 0.1 are significant at a significance level of $\alpha = 0.001$ (even when using the effective sample sizes, n', in order to account for autocorrelation; n' is always > 100). However, significance does not necessarily imply that the variable is a useful predictor since the amount of explained variance may be low. Furthermore, certain variable pairs are necessarily strongly correlated: such as D_s and V_s, or D_{500} and V_{500}, because of the way divergence is defined. Strong correlations are also expected *a priori* between T_{max} and T_{min}, and between q and both T_{max} and (especially) T_{min} given the temperature dependency of the saturation specific humidity. These variable pairs aside, the strongest DJF correlations were between H_{500} and T_{max}/T_{min}, H_{500} and q, Z_s and mslp, and the equivalent upper atmosphere correlation between Z_{500} and H_{500}. The same or stronger correlations occur in JJA, with the exception of the weaker correlation between T_{max} and q. Additional strong correlations that are either non-existent or noticeably weaker in DJF occur between F_{500} and H_{500}, T_{max} and F_{500} (partly because of high correlations between T_{max} and H_{500}, and F_{500} and H_{500}), q and D_s, q and V_s (because of the strong V_s–D_s link), and T_{min} and D_s (arising partly through the correlations between T_{min} and q, and q and D_s).

Overall, the inter-variable correlation strengths for observed and HadCM2 daily data were remarkably similar in both seasons providing a strong indication of the GCM's internal consistency and realism relative to the real world. In terms of explained variance the most notable differences occur in the correlations between: T_{max} and T_{min} (both seasons, with the GCM showing a stronger link in JJA and a weaker link in DJF); T_{max} and H_{500} (DJF, GCM correlation weaker); T_{min} and q (JJA, GCM correlation weaker); T_{min} and V_s (JJA, GCM correlation stronger); T_{min} and H_{500} (DJF, GCM correlation weaker); q and V_s and D_s (JJA, GCM correlations stronger); and q and H_{500} (GCM correlation weaker). Thus, the inter-variable correlation skill of the GCM was generally greater in DJF than in JJA.

3.2. Propinquitous precipitation relationships

The above results show how the choice of downscaling predictors may be complicated by differences in the relative strengths in the correlations involving observed data versus those for GCM data, and by covariances amongst the predictors. Keeping these issues in mind, Table V shows the power of each predictor variable in 'explaining' variations in O_i and R_i in terms of the squared correlation coefficients for all sites and seasons combined, comparing observed and HadCM2 data. In general, the highest explained variances for observed data are in winter, and explained variances tend to be higher for O_i than

Copyright © 2000 Royal Meteorological Society

Table IV. Strongest inter-variable correlations on a daily time-scale for the current climate

Variable pair		DJF		JJA	
		Observed	HadCM2	Observed	HadCM2
T_{max}	T_{min}	**0.87**	**0.77**	**0.65**	**0.81**
	q	**0.69**	**0.73**	**0.32**	**0.21**
	D_s	−0.37	−0.38	−0.28	−0.41
	H_{500}	**0.71**	**0.60**	**0.81**	**0.84**
	F_{500}	−0.21	0.03	**−0.55**	**−0.50**
	Z_{500}	−0.32	−0.27	−0.46	−0.48
T_{min}	q	**0.79**	**0.79**	**0.82**	**0.59**
	V_s	0.33	0.41	0.52	0.65
	D_s	−0.37	−0.47	**−0.58**	**−0.67**
	H_{500}	**0.62**	**0.44**	**0.73**	**0.75**
	Z_{500}	−0.27	−0.29	−0.33	−0.44
q	V_s	0.29	0.36	**0.48**	**0.62**
	D_s	−0.33	−0.43	**−0.52**	**−0.63**
	H_{500}	**0.49**	**0.49**	**0.48**	**0.32**
D_s	V_s	**−0.88**	**−0.87**	**−0.89**	**−0.91**
	H_{500}	−0.40	−0.33	−0.39	−0.45
	Z_{500}	0.47	0.45	0.29	0.30
Z_s	mslp	**−0.55**	**−0.55**	**−0.55**	**−0.56**
H_{500}	V_s	0.37	0.30	0.34	0.47
F_{500}	H_{500}	−0.28	−0.15	**−0.60**	**−0.54**
	U_{500}	0.31	0.25	0.36	0.43
D_{500}	mslp	0.38	0.44	0.17	0.29
	V_{500}	**−0.87**	**−0.88**	**−0.85**	**−0.85**
Z_{500}	V_s	−0.41	−0.40	−0.24	−0.30
	H_{500}	**−0.63**	**−0.56**	**−0.64**	**−0.62**

The pairs listed are the top 25 when ranked according to the overall strength of correlations, with all regions, both seasons and both data sources combined. Correlations in bold are discussed in the main body text.

for R_i. These results do not indicate weaknesses in the potential for statistical downscaling but, rather, the relative importance of the stochastic and deterministic components in any such downscaling scheme. Essentially, the correlations represent the amount of variability in O_i or R_i that may be explained by a deterministic regression equation. In statistical downscaling, a common method is to simulate the remaining variability stochastically (see, for example, Wilby *et al.*, 1998b).

The explained variances define those predictor variables that are likely to be most useful. The largest percentages of variance in observed O_i are explained by q, T_{max} (JJA) or T_{min} (DJF), mslp, U_s, H_{500} (and its correlate, V_{500}) and D_{500}. For observed R_i, the most important predictors are q (DJF only), T_{max} (JJA) or T_{min} (DJF), D_s, H_{500} (and its correlate, V500). Note that q covaries strongly with temperature, so the T_{max} and T_{min} relationships may largely reflect primary linkages with q.

In comparison, for HadCM2 the two strongest predictors overall are q and D_s. Except for O_i in DJF for q, these linkages are always stronger in the GCM than in the observed data. Conversely, almost all linkages with 500 hPa variables are weaker in the GCM than in the observations. These differences between how strongly precipitation depends on moisture and circulation predictors, observations versus model, point to possible deficiencies in the way the precipitation process is quantified in the model (although part of the difference here may reflect inadequacies in the way we have defined area-average precipitation in the observations).

Copyright © 2000 Royal Meteorological Society

Table V shows the overall precipitation–predictor relationships. It is also informative to examine spatial variations in the relative strength of the 15 predictors within both observed and HadCM2 data. Accordingly, Figures 2–5 show, by region, correlation coefficients between the various predictors and the equivalent observed and HadCM2 precipitation. Perfect agreement in the correlations obtained from observed and HadCM2 data would result in the 15 points lying on the 1:1 line. Large departures, either above or below this line, highlight discrepancies in the realism of the GCM–precipitation relationships. For example, Figure 2 indicates that HadCM2 slightly underestimates the positive influence of U_s on wintertime wet-day occurrence (O_i) at the two most western locations (SLM and SNV), and significantly understates the negative effect of D_{500} at all sites. Similarly, the relationship between V_{500} or Z_s and wintertime O_i is mostly weaker in HadCM2, whereas the correlation with T_{min} is overly strong relative to observations.

Similar diagnostic results are presented in Figures 3–5. For summertime O_i, Figure 3 suggests that the strength of the correlations with q are significantly exaggerated in HadCM2, whilst correlations with the circulation indices Z_s, V_{500} and D_{500} are too weak. The serious discrepancies in the HadCM2 correlations between precipitation and D_s, U_s, F_{500} and Z_{500} at SNV are particularly noteworthy.

Observed T_{max} is the variable that is most negatively correlated with precipitation at SLM, SNV and OKC. However, temperature–precipitation correlations are difficult to interpret, given that high summer temperatures may be symptomatic of clear skies and lower rainfall probabilities (i.e. a consequence rather than a cause of dry conditions). Conversely, in other regions high summer temperatures may imply more convective activity.

Figure 4 indicates that the strengths of correlations with D_{500} and Z_s are underestimated for wintertime R_i in HadCM2. In contrast, HadCM2 exaggerates the magnitude of (negative) correlations with D_s and Z_{500}, and (positive) correlations with F_s when compared with observed data. Finally, Figure 5 once again demonstrates that for summertime R_i, HadCM2 significantly exaggerates the magnitude of correlations with q. The general scatter in the points shown in Figure 5 suggests that, qualitatively, correlations between grid box predictors and grid box rainfall amounts are least realistically modelled by HadCM2 at the chosen sites in summer.

Table V. Mean percentage of variance in observed grid box daily precipitation occurrence (O_i) and wet-day amounts (R_i) explained by observed grid box predictor variables (all sites combined)

	Predictor/season			
	O_i/DJF	O_i/JJA	R_i/DJF	R_i/JJA
Lag-1	**12.2 (11.7)**	**10.3 (19.4)**	4.7 (6.1)	2.8 **(13.3)**
q	**12.6** (8.6)	6.0 **(13.5)**	**10.6 (11.2)**	1.4 **(15.1)**
T_{max}	1.8 (4.5)	**11.1** (7.5)	2.2 (5.7)	9.1 **(14.5)**
T_{min}	**10.8 (15.3)**	3.9 (4.1)	8.4 **(16.0)**	1.5 (5.2)
mslp	**10.4** (4.5)	5.2 (1.9)	6.0 (4.7)	3.6 (2.5)
U_s	**12.7** (8.8)	6.9 (5.8)	5.3 (7.9)	2.2 (5.0)
V_s	6.2 (6.1)	4.7 (7.6)	6.7 **(10.4)**	5.1 (7.6)
F_s	2.0 (2.2)	1.5 (6.1)	7.2 **(18.2)**	1.3 (2.7)
Z_s	6.0 (2.5)	7.3 (4.8)	2.1 (1.1)	2.2 (1.5)
D_s	5.9 (6.4)	5.8 **(10.6)**	**10.6 (19.9)**	5.9 (9.1)
H_{500}	6.1 (5.3)	8.5 (5.3)	2.3 (3.9)	4.5 (6.0)
U_{500}	3.0 (6.0)	3.8 (3.0)	2.4 (3.6)	1.3 (3.3)
V_{500}	**16.6** (7.1)	5.5 (2.7)	**10.4** (9.1)	3.5 (1.2)
F_{500}	4.3 (2.8)	1.8 (2.4)	4.7 (3.5)	1.6 (2.4)
Z_{500}	2.0 (2.1)	4.7 (8.3)	2.7 (6.5)	1.4 (1.8)
D_{500}	**15.5** (5.4)	5.9 (2.7)	**10.2** (6.5)	4.6 (1.5)

Corresponding results for HadCM2 are shown in parentheses. For comparative purposes, the percentage of variance explained by the lag-1 predictand is also included. The most powerful predictors (>10% explained variance) are highlighted in bold.

Copyright © 2000 Royal Meteorological Society

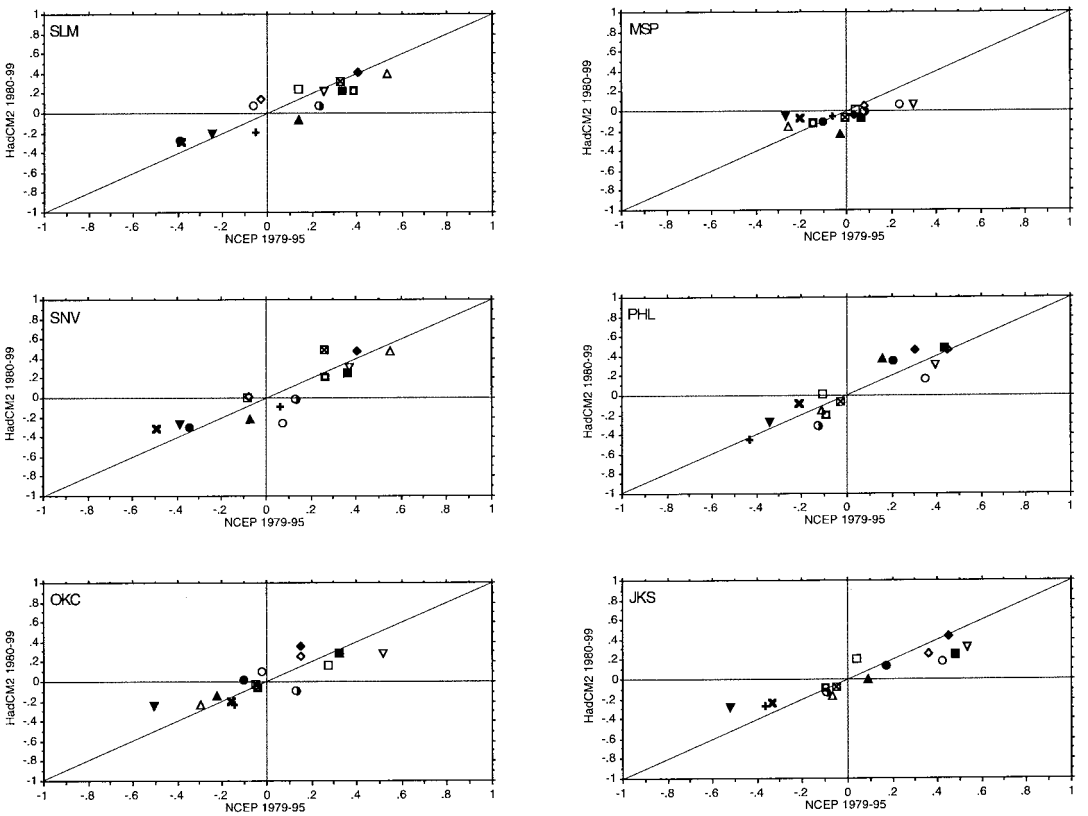

Figure 2. The strength of relationships between daily grid box predictors and winter wet-day/dry-day sequences, O_i: observed (NCEP re-analysis) versus HadCM2 1980–1999 correlation coefficients. ○, Z_s; □, F_s; △, U_s; ◇, V_s; +, D_s; ⊠, mslp; ■, q; ▲, T_{max}; ◆, T_{min}; ●, H_{500}; ◑, Z_{500}; ▣, F_{500}; ⊡, U_{500}; ▽, V_{500}; ▼, D_{500}

3.3. Spatial correlation patterns for mslp

Figures 6 and 7 show the spatial patterns of correlation between daily precipitation (O_i and R_i) and mslp at SNV and OKC in observed and HadCM2 data, for winter and summer, respectively. Following McCabe and Dettinger (1995), regions of negative correlation are assumed to represent areas of anomalous (i.e. enhanced) cyclonic circulation, while the direction of the isolines over the target region represents the time-averaged (anomalous) storm tracks. In general, the spatial distributions of correlations produced by HadCM2 are very similar to observed distributions in terms of the patterns, locations of maxima and alignment of isolines.

Figure 6 shows that for winter precipitation occurrence (O_i) at SNV in both observed and HadCM2 data, maximum negative correlations lie to the north and northwest, implying that the greatest likelihood of precipitation is associated with a predominantly westerly flow over the target region. In the case of OKC, the domain of the maximum correlation lies to the southwest with isolines aligned in a prominent southeast–northwest direction.

For precipitation amount (R_i), although the locations of the maximum DJF correlations with mslp are broadly similar for observed and HadCM2 precipitation amounts, the HadCM2 patterns at SNV are slightly stronger and cover a larger spatial domain than in the observations. At OKC, HadCM2 identifies an area of weak positive correlations to the northeast of the target region over the Great Lakes that is absent in observed data (Figure 6, bottom two panels). From Figure 6, it is also evident that there are differences between the correlation fields for daily R_i and O_i, but these are quite subtle and may merely represent the effects of statistical uncertainty. For example, winter R_i at SNV correlates with airflows from a more southerly trajectory than O_i.

Copyright © 2000 Royal Meteorological Society

As might be anticipated from the greater influence of convective processes in JJA, the correlations for summer O_i and R_i (Figure 7) are generally weaker and more spatially heterogeneous than in the winter case for both the observed and HadCM2 patterns. The location of the maximum correlation, the spatial extent and the alignment of the maximum gradient have also shifted slightly relative to DJF (to the southwest in the case of SNV and to the east for OKC). However, once again, the level of correspondence between the observed and HadCM2 patterns is encouraging.

3.4. Spatial correlation patterns for q

Figures 8 and 9 show the correlation fields between daily precipitation and specific humidity in winter and summer, respectively. For winter (Figure 8), the strength and spatial distribution of the correlations are remarkably similar for O_i and R_i. Observed and HadCM2 results are also very similar. The greater propinquity of the maximum correlations to the target sites (compared with the cases for mslp) is noteworthy. The summer situation (Figure 9), however, reveals significant differences between observed and HadCM2 precipitation correlations. For example, at SNV, HadCM2 returns stronger correlations for both O_i and R_i relative to observed conditions. Whereas the observed data imply little or no correlation between daily q and daily R_i, HadCM2 suggests that q could account for approximately 20% of the variance in daily wet-day amounts at this site. Similarly, at OKC the maximum correlations and spatial extent of the positive correlation field produced by HadCM2 are much greater than in observed data. This larger influence of specific humidity on precipitation in the GCM relative to the observations was noted earlier. It may point to some oversimplifications in the model physics controlling both the amounts and frequency of precipitation.

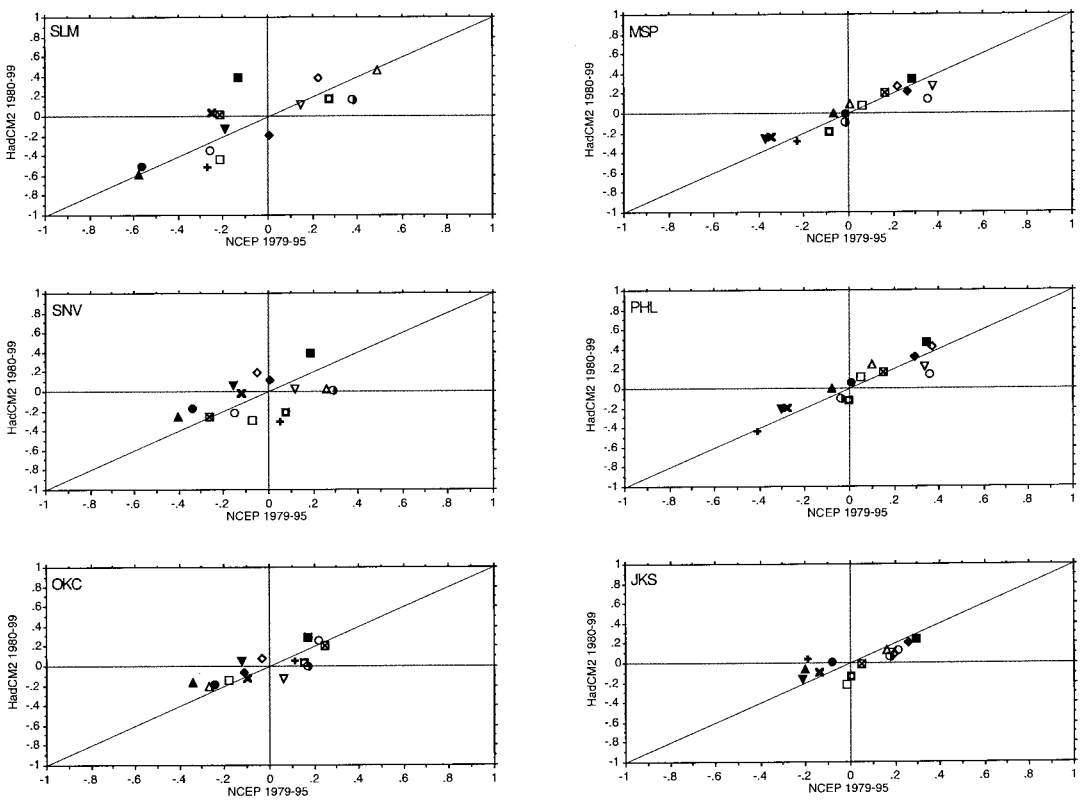

Figure 3. The same as Figure 2, but for summer wet-day/dry-day sequences, O_i

Copyright © 2000 Royal Meteorological Society

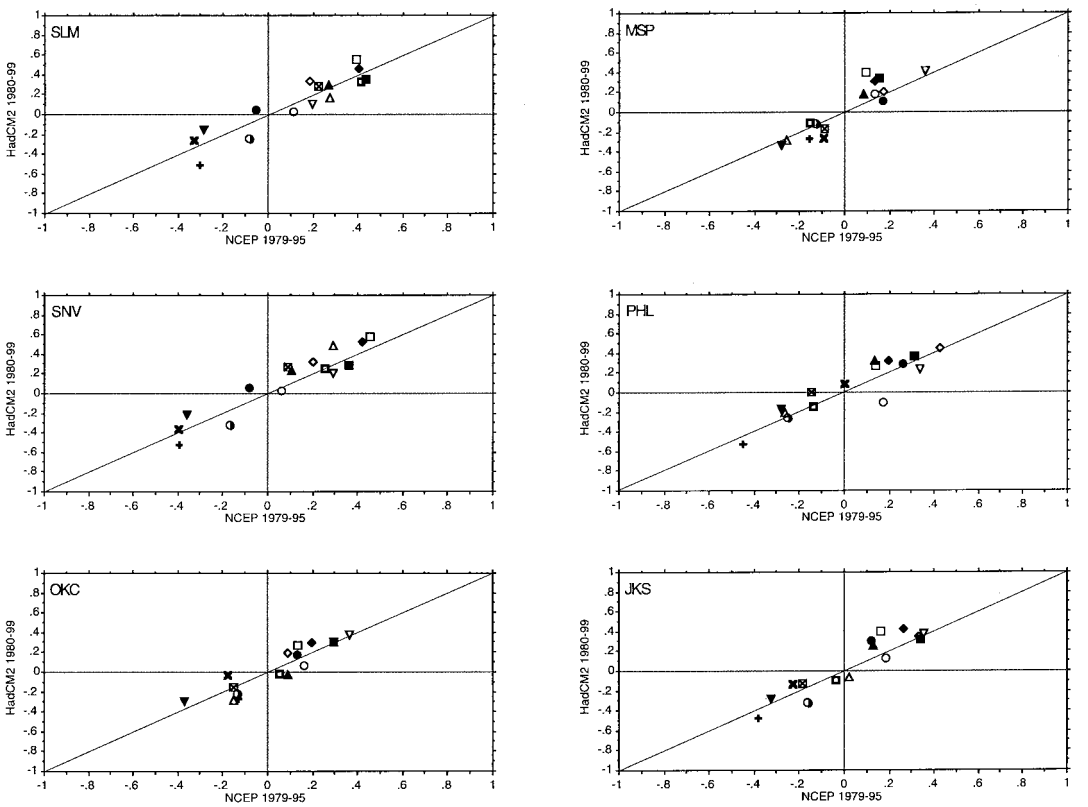

Figure 4. The same as Figure 2, but for winter wet-day amount sequences, R_i

4. DISCUSSION

Before evaluating the significance of the preceding results to statistical downscaling, some caveats should be noted. First, the HadCM2 1980–1999 climate scenario is unlikely to be a faithful representation of the present-day observed (1979–1995) climate. Wilby *et al.* (1998b) noted that even though the model simulation begins in the year 1861, the initial state of the ocean in the HadCM2 SUL experiment does not correspond to 1861 conditions (rather, 'present-day' ocean temperatures were employed). Furthermore, changes in atmospheric forcing from 1861 onwards do not correspond precisely to real-world changes. For model years 1980–1999 the SUL run partially simulates historical aerosol forcing effects, but has a CO_2 level that corresponds to conditions anticipated around 2020–2040. As a result of this, in none of the experiments performed with HadCM2 is the present-day climate simulated in a fully consistent way. The validation of HadCM2 against observed data, as performed here, therefore rests on the assumptions that the various relationships between variables that we have evaluated remain reasonably constant with time as the climate state changes. This is judged to be a reasonable and physically well-founded assumption. It has, furthermore, been tested to a limited extent by comparing precipitation–mslp relationships in 2080–2099, with those in 1980–1999 (see below). Future and 'present-day' relationships are identical within statistical sampling uncertainty.

Second, it has been assumed that the unweighted five-station, areal mean of daily observed precipitation is a 'true' grid box mean that can legitimately be compared with results for the HadCM2 grid. In fact, results from the Atmospheric Model Intercomparison Project (Gates *et al.*, 1999) suggest that the direct use of station data, as performed in this experiment, will tend to underestimate the frequency of grid box-area rain days (Osborn and Hulme, 1998). This effect is most pronounced in summer when average correlation decay lengths between pairs of stations in a grid box are lower due to the predominance of

Copyright © 2000 Royal Meteorological Society

convective precipitation events (Osborn and Hulme, 1997). This denotes a failure to identify 'marginal' wet-days (i.e. those days where rainfall occurs over a relatively small area of the grid box, between stations), which in turn will lead to a slight bias in the O_i and R_i samples used for the correlation analyses. However, the fact that the HadCM2 and observed correlation fields shown in Figures 6 and 7 are so similar, for two contrasting regions, suggests that this problem is relatively minor.

For the application of statistical downscaling results to future, GCM-simulated climate, the following are required: reasonable fidelity (at least) of the model in terms of inter-variable relationships and relationships between precipitation characteristics and predictor variables; and long time-scale stability of precipitation-predictor relationships. The correlation analyses (Table IV) have shown that the GCM used here reproduces well most of the observed correlations between potential predictor variables at the grid box level and daily time-scale. There were no cases where a strong relationship in the observed data was not reflected in the HadCM2 data, or *vice versa*. There were, however, a number of cases where the strengths of relationships differed noticeably, particularly in JJA. In spite of these differences, these results are considered to be a strong endorsement of the physical realism of the model.

In terms of precipitation–predictor relationships (Table V), there are a number of differences between observations and the model: First, in JJA, both O_i (precipitation occurrence) and R_i (wet-day amount) are far more dependent on atmospheric moisture level (q) in the GCM than in the real world. This result probably arises from oversimplifications in the GCM's modelling of the precipitation process.

Second, in DJF, both precipitation variables have much stronger relationships with $T_{\min}$ in the model than in the observations. In addition, surface divergence (D_s) is a stronger predictor in the model (especially for R_i in DJF and O_i in JJA), a result reflected in the surface meridional wind component (V_s) by virtue of the necessarily strong D_s–V_s correlation. The model also displays a stronger link between precipitation (both O_i and R_i) and geostrophic wind speeds at the surface than in the observations. It is

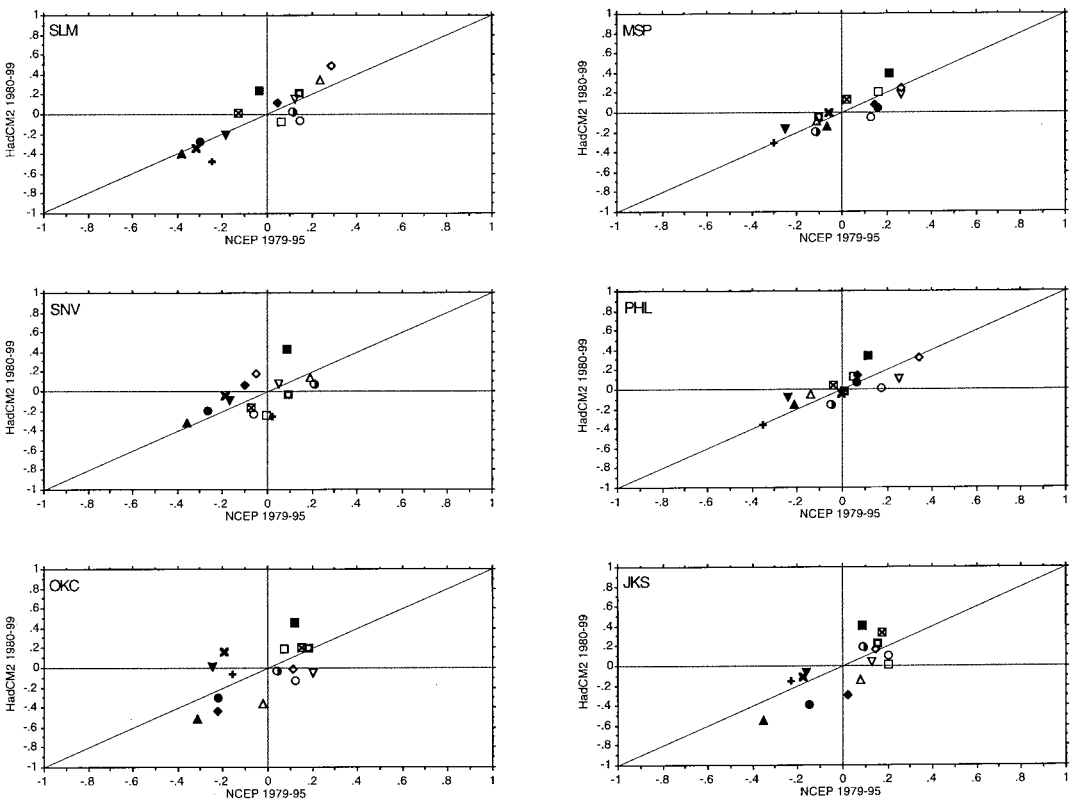

Figure 5. The same as Figure 2, but for summer wet-day amount sequences, R_i

Copyright © 2000 Royal Meteorological Society

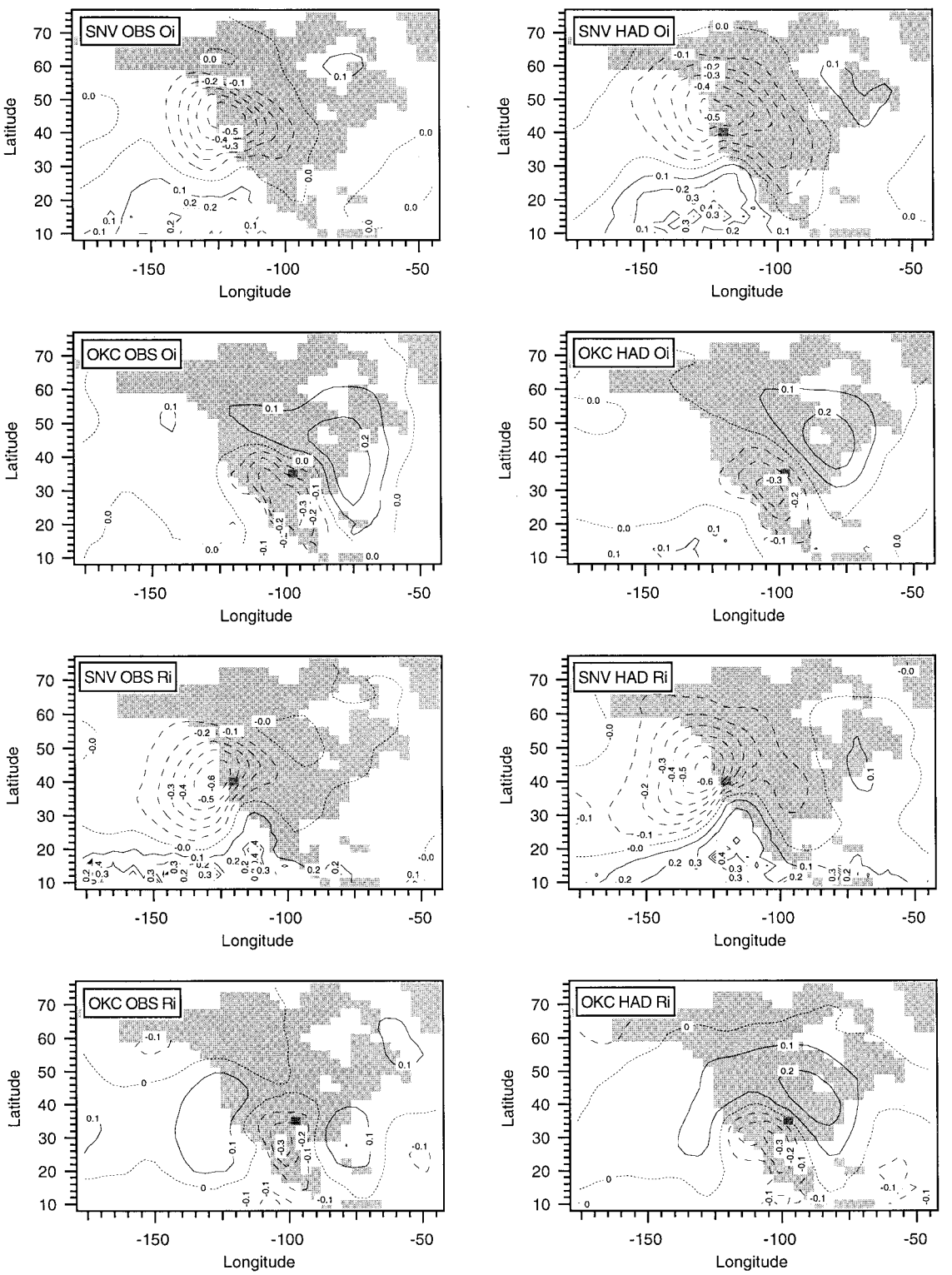

Figure 6. Correlations for winter between daily mslp versus daily precipitation occurrence (O_i) and amount sequences (R_i) at SNV and OKC, based on observed data (1979–1995) and simulations from HadCM2 (1980–1999)

Copyright © 2000 Royal Meteorological Society

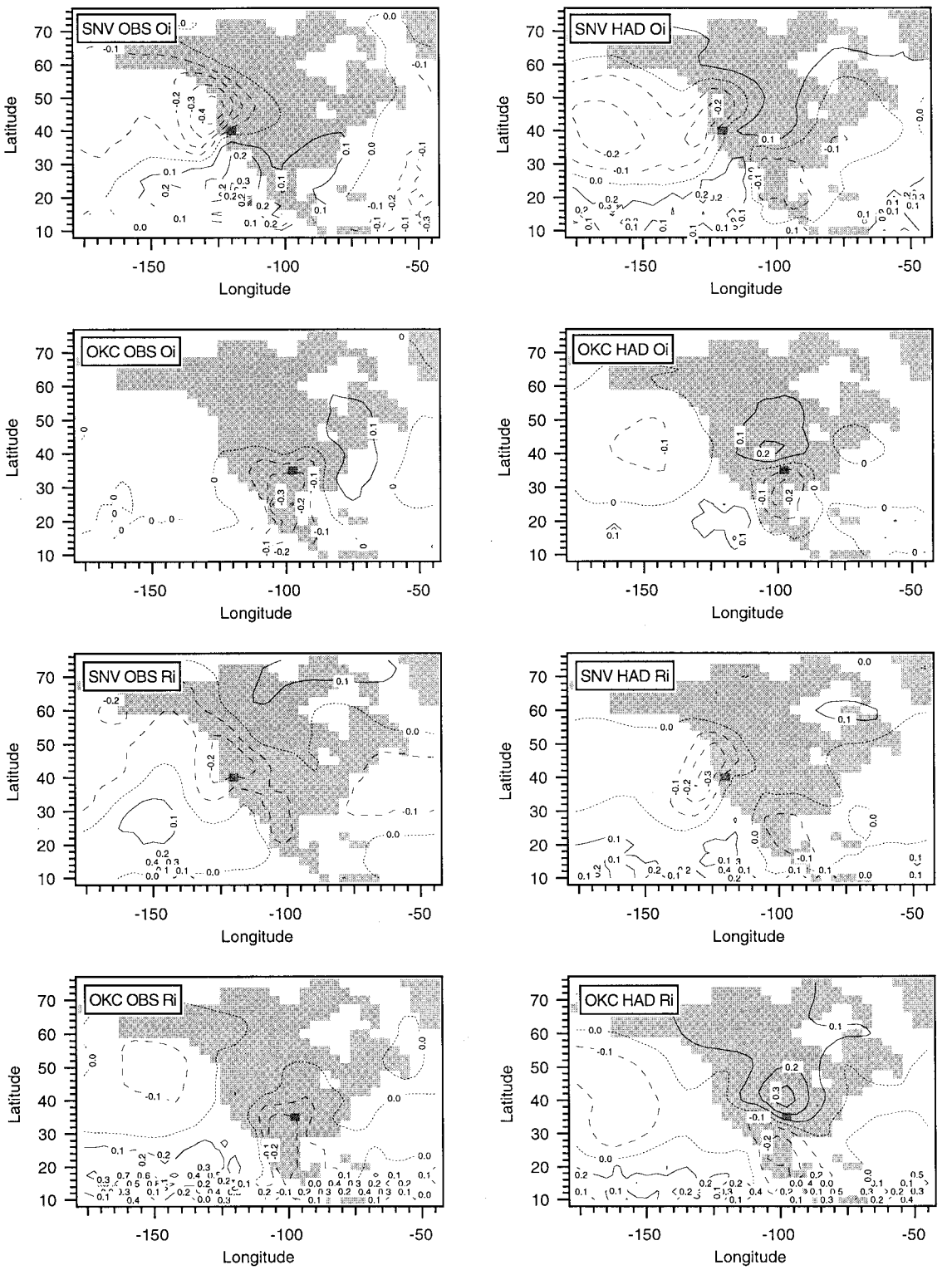

Figure 7. The same as Figure 6, but for summer

Copyright © 2000 Royal Meteorological Society

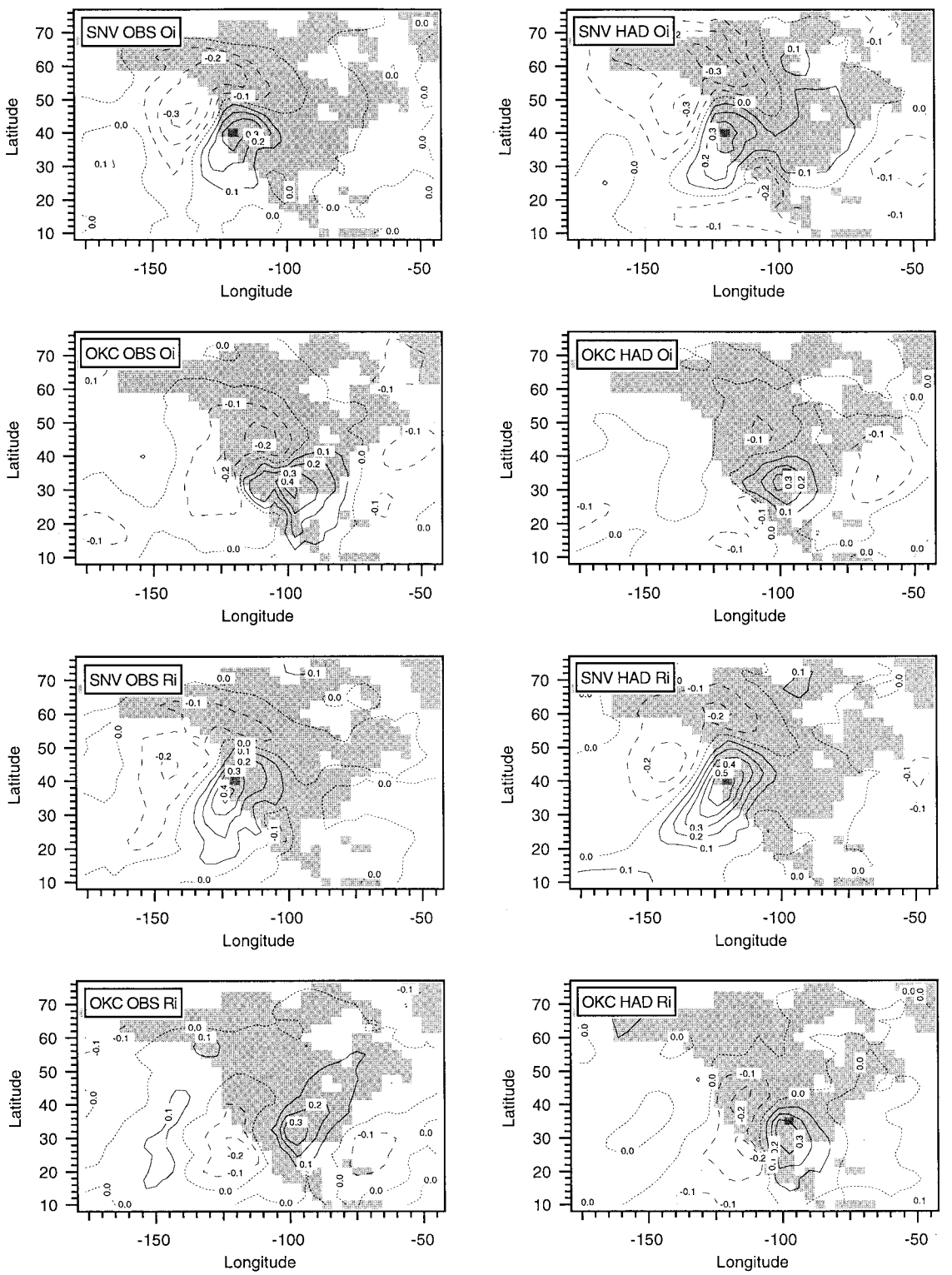

Figure 8. Correlations for winter between daily specific humidity versus daily precipitation occurrence (O_i) and amount sequences (R_i) at SNV and OKC, based on observed data (1979–1995) and simulations from HadCM2 (1980–1999)

Copyright © 2000 Royal Meteorological Society

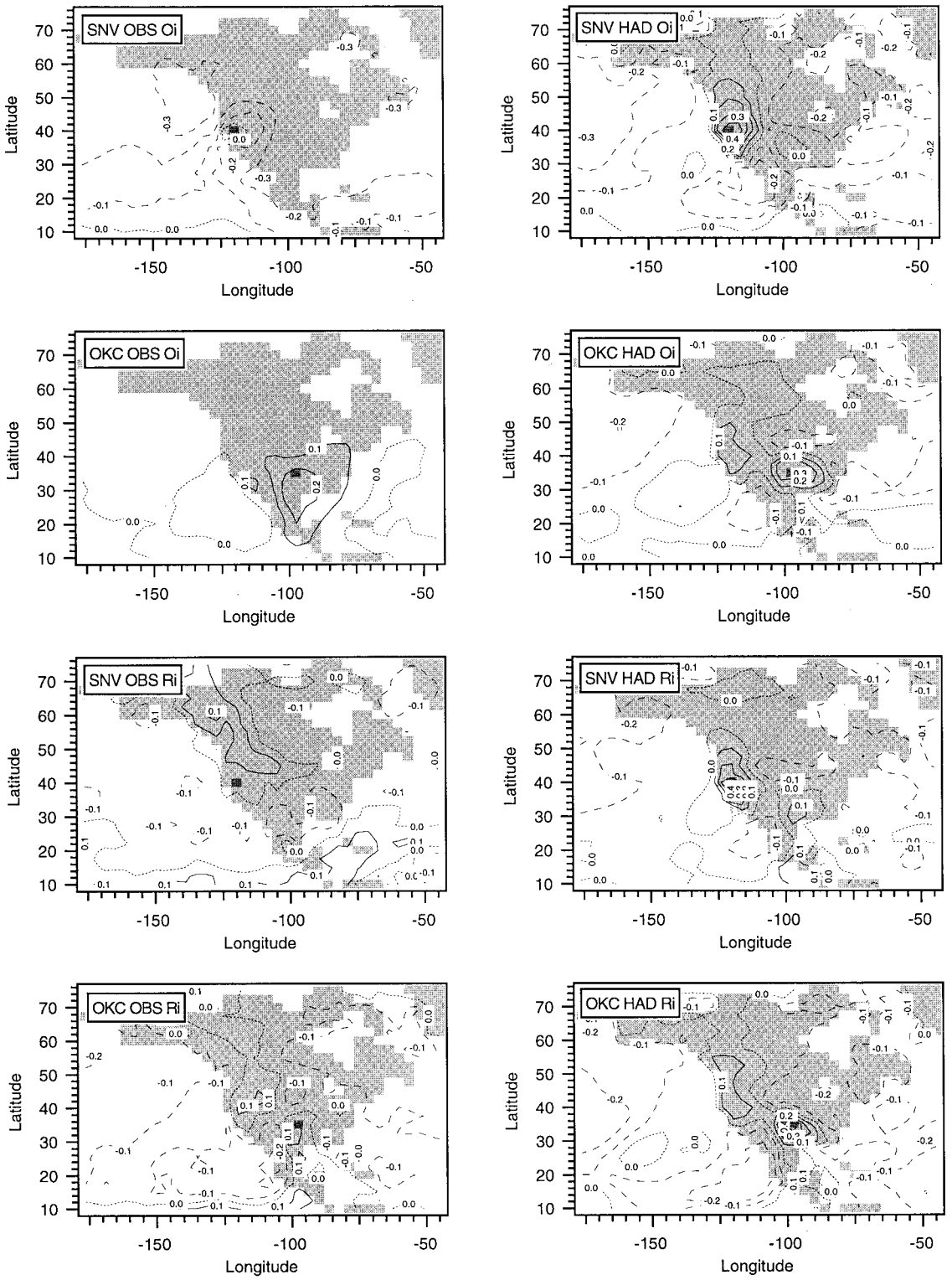

Figure 9. The same as Figure 8, but for summer

Copyright © 2000 Royal Meteorological Society

likely that these results arise from differences in orography between the model and the real world—if so, one might expect higher resolution models to give results that bear a greater resemblance to the observations. (Some of these differences may also arise from the relative crudeness of our observed 'grid box' precipitation estimates, noted above.)

Third, for O_i in DJF, 500 hPa divergence (D_{500}) (and the closely-related variable V_{500}) is a much stronger predictor variable in the observed data than in the model. Mean sea-level pressure (mslp) (which is related to D_{500} in DJF—see Table IV) is also a stronger observed predictor than in the model. It is suspected that these are differences that arise from deficiencies in model physics. The mslp case, however, appears to reflect only a very minor difference between model and observed O_i–mslp relationships. At OKC, propinquitous relationships are very similar (Figure 6). At SNV, the observed propinquitous relationship is stronger than in the GCM, but only by virtue of a slight offset in the spatial pattern of correlations (Figure 6, top two panels).

Finally, both O_i and R_i are much more strongly autocorrelated in JJA in the GCM than in the real world (Table V). The reason for this persistence is unclear, given that it is not evident in DJF. It is possible that the split between convective and large-scale precipitation in the model is unrealistic; no access to appropriate model data in order to test this hypothesis was possible in this case.

Overall, the results shown in Table V highlight the importance of atmospheric circulation in the provision of conditions necessary for precipitation to occur in both the model and the real world, and of atmospheric moisture content in the provision of the source material. No single variable is a dominant predictor variable, however, implying that multivariate prediction equations are essential in order to produce high quality downscaling schemes. Table V also shows that, in some instances, indirect predictors can be of considerable value (such as temperature as a proxy for atmospheric moisture content).

In terms of model performance, the most striking result is the much stronger dependence of model precipitation on atmospheric moisture content in JJA compared with observations, especially at the SNV site. This is illustrated in Figure 9 (compare the right-hand maps of the GCM correlation patterns with the left-hand column of observed correlations). Given these results, it is not surprising that the GCM yields significant increases in precipitation under future, warmer climate scenarios (Johns *et al*., 1997). These increases contrast with the relatively modest changes in precipitation arising from circulation-based downscaling methods (Wilby and Wigley, 1997). This outcome is also a function of the relative insensitivity of circulation indices produced by HadCM2 to future radiative forcing (Wilby *et al*., 1998a).

A fundamental assumption made in statistical downscaling is temporal stability of predictor variable relationships. By way of an example, Figure 10 shows the HadCM2 correlation distributions for relationships between mslp and both precipitation occurrence and amounts at SNV and OKC, for the period 2080–2099. Comparing the distributions shown in Figure 10 with the HadCM2 simulations for 1980–1999 in Figure 6 (summer, cf. left panel of Figure 10) and Figure 7 (winter, cf. right panel of Figure 10) shows that for mslp as a predictor, relationships with O_i or R_i are indeed stationary even though the model's overall climate in 2080–2099 differs markedly from that in 1980–1999. These results imply that the strength of circulation–precipitation correlations in HadCM2 is unaffected by changes in other variables, such as temperature and specific humidity.

In many statistical downscaling studies, only propinquitous relationships are considered, i.e. no direct account is taken of possible spatial offsets in the correlation patterns between predictors and predictands. The results presented in Figures 6–9 show that such offsets do indeed exist. These figures provide insights into both the most appropriate focal point, and the predictor domain size(s) for downscaling. It is evident that the strength and spatial extent of the optimal predictor, for a given target precipitation region, vary both seasonally and geographically. For example, the centroid for the observed R_i versus mslp correlation for SNV in winter (Figure 6) is located approximately at 130°W, 40°N ($r = -0.6$) compared with 120°W, 45°N ($r = -0.2$) in summer (Figure 7). Furthermore, the use of gridded circulation predictors for the atmosphere directly overlying the target grid box consistently fails to capture the strongest correlations, as in observed winter R_i at OKC (Figure 6). This may account for the relatively low percentage of variance explained by daily precipitation models based on single grid box circulation predictors. In contrast, the optimal domain(s) for atmospheric moisture content tended to overlap with the target grid

Copyright © 2000 Royal Meteorological Society

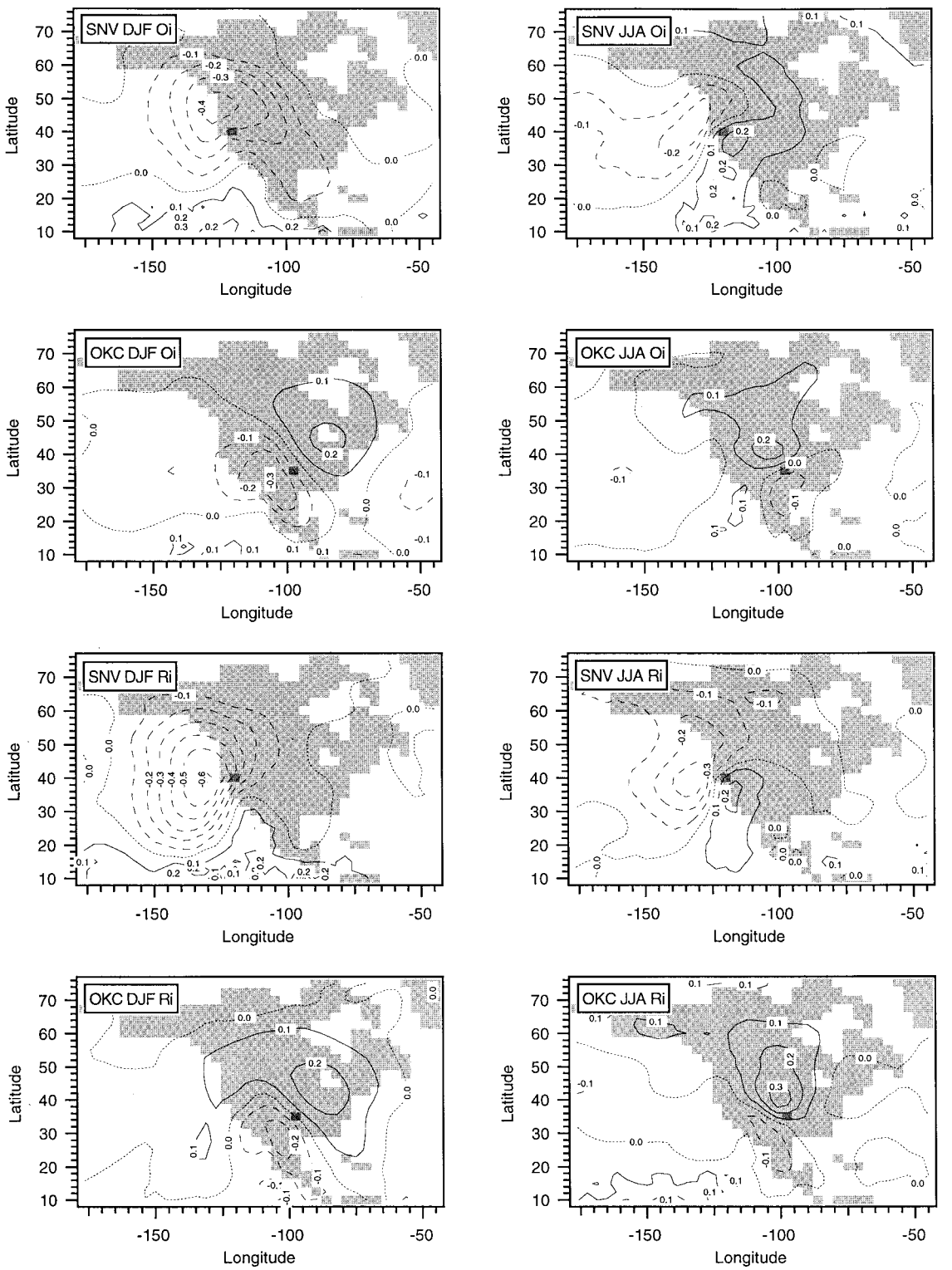

Figure 10. Winter and summer season correlations between daily mslp and daily precipitation occurrence (O_i) and amount sequences (R_i) at SNV and OKC, based on simulations from HadCM2 (2080–2099)

Copyright © 2000 Royal Meteorological Society

box and were geographically smaller in extent than the circulation domains (e.g. summer O_i at SNV, Figure 9).

Finally, it is often assumed in multivariate downscaling that the location and spatial extent of the predictor domain are the same for different predictors and different surface variables. As Figures 6–9 reveal, this may not necessarily be a valid assumption. For example, there are subtle differences in the observed correlation distributions between R_i and O_i at both sites. As noted previously, the optimal predictor domains also vary according to the choice of predictor variable, whether daily mslp (Figures 6 and 7) or daily moisture level (Figures 8 and 9).

5. CONCLUSIONS

Observed and HadCM2-simulated correlations between 15 explanatory variables and daily precipitation occurrence/amounts were examined using gridded data for six locations in the USA. Daily precipitation was chosen as the focus of the study because of its still problematic representation in statistical downscaling schemes. A focus of the study was the validation of the GCM in terms of inter-variable correlations and correlations between precipitation and the suite of explanatory variables. For the former, model and observed correlations were generally similar: all high correlations in the observed data were reflected in high model correlations, and *vice versa*. These results provide a strong endorsement of the physical realism of the GCM.

Correlations involving precipitation were, however, less satisfactory. In line with previous research (e.g. Stidd, 1954; McCabe and Dettinger, 1995) observed correlations between grid box circulation indices and grid box daily precipitation were strongest at locations near oceanic sources in winter, where the advection of atmospheric moisture is important. However, the strengths of such circulation-based correlations differed between HadCM2 and the real world. At the surface, observed dependencies on mslp were stronger (especially for precipitation occurrence [O_i] in winter) while HadCM2 precipitation tended to show a stronger dependence on divergence (especially for precipitation amounts [R_i] in winter). At 500 hPa, observed precipitation was much more dependent on divergence than was model precipitation, particularly in winter. In all cases, the dependence of precipitation on vorticity, previously used as primary predictor in downscaling studies, was relatively weak. HadCM2 placed much greater emphasis on grid box specific humidity as the leading explanatory variable, especially in summer.

Given that circulation indices simulated by HadCM2 are less sensitive than atmospheric moisture content to future radiative forcing, it is expected that downscaling methods based on these two variable types should yield smaller changes in grid box precipitation than HadCM2. Such differences are likely to be greatest during summer when the correlation between precipitation and specific humidity is noticeably stronger in the GCM than in reality. The stronger dependence of model precipitation on specific humidity suggests that model precipitation changes might be overestimated. There is some danger, however, in extrapolating the present results, which are based on inter-annual variations, to the context of longer time-scale anthropogenic change.

In addition to the above propinquitous relationships, correlations between daily precipitation occurrence and amounts (O_i and R_i) and mslp and specific humidity remote from the precipitation site were also examined. The correlation patterns obtained for O_i at two grid boxes centred on the Sierra Nevada (SNV) and Oklahoma (OKC) were broadly similar for observed data and HadCM2 output. This suggests that, for the chosen sites at least, regional relationships between O_i and atmospheric circulation are captured realistically by HadCM2. However, the correlation patterns for wet-day amounts (R_i) were not so faithfully reproduced by HadCM2, particularly at OKC in summer. Similarly, differences between observed and HadCM2 correlation fields for specific humidity were greater in summer at both sites. These results imply that the choice of the predictor and its corresponding domain, in terms of location and spatial extent, may be critical factors affecting the realism and stationarity of downscaled precipitation scenarios. Further research is required to determine the generality of these findings for other regions, predictors, surface variables and GCMs.

Copyright © 2000 Royal Meteorological Society

ACKNOWLEDGEMENTS

This is an ACACIA (A Consortium for the Application of Climate Impact Assessments) contribution. ACACIA is sponsored by CRIEPI, EPRI, KEMA and NCAR. We are grateful to David Viner of the Climate Impacts LINK Project (UK Department of the Environment Contract EPG1/1/16) for supplying the HadCM2 data on behalf of the Hadley Centre and UK Meteorological Office. We thank Doug Lindholm for his assistance in acquiring the NCEP re-analysis data and an anonymous referee for constructive comments. The National Center for Atmospheric Research is sponsored by the National Science Foundation.

REFERENCES

Bardossy, A. and Plate, E.J. 1992. 'Space-time model for daily rainfall using atmospheric circulation patterns', *Water Resources Res.*, **28**, 1247–1259.

Charles, S.P., Bates, B.C., Whetton, P.H. and Hughes, J.P. 1999. 'Validation of downscaling models for changed climate conditions: case study of southwestern Australia', *Climate Res.*, **12**, 1–14.

Conway, D., Wilby, R.L. and Jones, P.D. 1996. 'Precipitation and airflow indices over the British Isles', *Climate Res.*, **7**, 169–183.

Crane, R.G. and Hewitson, B.C. 1998. 'Doubled CO_2 precipitation changes for the Susquehanna Basin: downscaling from the GENESIS General Circulation Model', *Int. J. Climatol.*, **18**, 65–76.

Department of the Environment (DOE), 1996. *Review of the Potential Effects of Climate Change in the United Kingdom*, HMSO, London.

Gates, W.L., Boyle, J., Covey, C., Dease, C., Doutriaux, C., Drach, R., Fiorino, M., Geckler, P., Hnilo, J., Marlais, S., Phillips, T., Potter, G., Santer, B.D., Sperber, K.R., Taylor, K. and Williams, D. 1999. *An Overview of the Results of the Atmospheric Model Intercomparison Project (AMIP)*, Vol. 80, Bureau of the American Meteorological Society, pp. 29–56.

Giorgi, F. and Mearns, L.O. 1991. 'Approaches to the simulation of regional climate change. A review', *Rev. Geophys.*, **29**, 191–216.

Goodess, C.M. and Palutikof, J.P. 1998. 'Development of daily rainfall scenarios for southeast Spain using a circulation-type approach tp downscaling', *Int. J. Climatol.*, **10**, 1051–1083.

Hay, L.E., McCabe, G.J., Wolock, D.M. and Ayers, M.A. 1992. 'Use of weather types to disaggregate General Circulation Model predictions', *J. Geophys. Res.*, **97**, 2781–2790.

Hennessy, K.J., Gregory, J.M. and Mitchell, J.F.B. 1997. 'Changes in daily precipitation under enhanced greenhouse conditions', *Climate Dynamics*, **13**, 667–680.

Hostetler, S.W. 1994. 'Hydrologic and atmospheric models: the (continuing) problem of discordant scales', *Clim. Change*, **27**, 345–350.

Hulme, M., Briffa, K.R., Jones, P.D. and Senior, C.A. 1993. 'Validation of GCM control simulations using indices of daily airflow types over the British Isles', *Climate Dynamics*, **9**, 95–105.

Huth, R. 1999. 'Statistical downscaling in central Europe: evaluation of methods and potential predictors', *Climate Res.*, **13**, 91–101.

Johns, T.C., Carnell, R.E., Crossley, J.F., Gregory, J.M., Mitchell, J.F.B., Senior, C.A., Tett, S.F.B. and Wood, R.A. 1997. 'The Second Hadley Centre coupled ocean-atmosphere GCM: Model description, spinup and validation', *Climate Dynamics*, **13**, 103–134.

Jones, P.D., Hulme, M. and Briffa, K.R. 1993. 'A comparison of Lamb Circulation Types with an objective classification scheme', *Int. J. Climatol.*, **13**, 655–663.

Kalnay, E., Kanamitsu, M., Kistler, R., Collins, W., Deaven, D., Gandin, L., Iredell, M., Saha, S., White, G., Woollen, J., Zhu, Y., Chelliah, M., Ebisuzaki, W., Higgins, W., Janowiak, J., Mo, K.C., Ropelewski, C., Wang, J., Leetmaa, A., Reynolds, R., Jenne, R. and Joseph, D. 1996. 'The NCEP/NCAR 40-year reanalysis project', *Bull. Am. Meteorol. Soc.*, **77**, 437–471.

Karl, T.R., Wang, W.C., Schlesinger, M.E., Knight, R.W. and Portman, D. 1990. 'A method of relating General Circulation Model simulated climate to the observed local climate. Part I: Seasonal statistics', *J. Climate*, **3**, 1053–1079.

Katz, R.W. and Parlange, M.B. 1996. 'Mixtures of stochastic processes: application to statistical downscaling', *Climate Res.*, **7**, 185–193.

Kilsby, C.G., Cowpertwait, P.S.P., O'Connell, P.E. and Jones, P.D. 1998. 'Predicting rainfall statistics in England and Wales using atmospheric circulation variables', *Int. J. Climatol.*, **18**, 523–539.

Kim, J.W., Chang, J.T., Baker, N.L., Wilks, D.S. and Gates, W.L. 1984. 'The statistical problem of climate inversion: determination of the relationship between local and large-scale climate' *Monthly Weather Rev.*, **112**, 2069–2077.

Klein, W.H. 1963. 'Specification of precipitation from the 700 millibar circulation', *Monthly Weather Rev.*, **91**, 527–536.

Matyasovszky, I. and Bogardi, I. 1996. 'Downscaling two versions of a general circulation model to estimate local hydroclimatic factors under climate change', *Hydrol. Sci. J.*, **41**, 117–129.

McCabe, G.J. and Dettinger, M.D. 1995. 'Relations between winter precipitation and atmospheric circulation simulated by the Geophysical Fluid Dynamic Laboratory General Circulation Model', *Int. J. Climatol.*, **15**, 625–638.

Mitchell, J.F.B. and Johns, T.C. 1997. 'On modification of global warming by sulphate aerosols', *J. Climate*, **10**, 245–267.

Osborn, T.J. and Hulme, M. 1997. 'Development of a relationship between station and grid box rainday frequencies for climate model evaluation', *J. Climate*, **10**, 1885–1908.

Osborn, T.J. and Hulme, M. 1998. 'Evaluation of the European daily precipitation characteristics from the Atmospheric Model Intercomparison Project', *Int. J. Climatol.*, **18**, 505–522.

Perica, S. and Foufoula-Georgiou, E. 1996. 'A model for multiscale disaggregation of spatial rainfall based on coupling meteorological and scaling descriptions', *J. Geophys. Res.*, **101**, 26347–26361.

Copyright © 2000 Royal Meteorological Society

Pilling, C., Wilby, R.L. and Jones, J.A.A. 1998. 'Downscaling of catchment hydrometeorology from GCM output using airflow indices in upland Wales', in: Wheater, H. and Kirby, C. (eds), *Hydrology in a Changing Environment*, Vol. 1, Wiley, Chichester, pp. 191–208.

Richards, J.M. 1971. 'Simple expression for the saturation vapour pressure of water in the range − 50° to 140°', *Brit. J. Appl. Phys.*,**4**, L15–L18.

Stidd, C.K. 1954. 'The use of correlation fields in relating precipitation to circulation', *J. Meteorol.*, **11**, 202–213.

von Storch, H., Zorita, E. and Cubasch, U. 1993. 'Downscaling of global climate change estimates to regional scales: an application to Iberian rainfall in wintertime', *J. Climate*, **6**, 1161–1171.

Wigley, T.M.L., Jones, P.D., Briffa, K.R. and Smith, G. 1990. 'Obtaining sub-grid-scale information from coarse resolution general circulation model output', *J. Geophys. Res.*, **95**, 1943–1953.

Wilby, R.L. 1998. 'Statistical downscaling of daily precipitation using daily airflow and seasonal teleconnection indices', *Climate Res.*, **10**, 163–178.

Wilby, R.L. and Wigley, T.M.L. 1997. 'Downscaling General Circulation Model output: a review of methods and limitations', *Prog. Phys. Geogr.*, **21**, 530–548.

Wilby, R.L., Hassan, H. and Hanaki, K. 1998a. 'Statistical downscaling of hydrometeorological variables using general circulation model output', *J. Hydrol.*, **205**, 1–19.

Wilby, R.L., Wigley, T.M.L., Conway, D., Jones, P.D., Hewitson, B.C., Main, J., and Wilks, D.S. 1998b. 'Statistical downscaling of General Circulation Model output: a comparison of methods', *Water Resources Res.*, **34**, 2995–3008.

Wilks, D.S. 1992. 'Adapting stochastic weather generation algorithms for climate change studies', *Climat. Change*, **22**, 67–84.

Woodhouse, C.A. 1997. 'Winter climate and atmospheric circulation patterns in the Sonoran desert region, USA', *Int. J. Climatol.*, **17**, 859–873.

Copyright © 2000 Royal Meteorological Society